Calcium uncaging with visible light.

HK Agarwal[1,2], R. Janicek[2,3], SH Chi[4], JW Perry[4], E. Niggli[3]*, and GCR Ellis-Davies[1]*.

[1] Department of Neuroscience,
Mount Sinai School of Medicine,
New York,
NY 10029,
USA.

[3] Department of Physiology,
University of Bern,
Bern CH 3012,
Switzerland.

[4]School of Chemistry and Biochemistry,
Center for Organic Photonics and Electronics,
Georgia Institute of Technology,
Atlanta,
GA 30332,
USA.

* correspondence graham.davies at mssm.edu or niggli at pyl.unibe.ch.
[2] these authors contributed equally to this work.

Abstract.

We have designed a nitroaromatic photochemical protecting group that absorbs visible light in the violet-blue range. The chromophore is a dinitro derivative of bisstyrylthiophene (or BIST) that absorbs light very effectively (ε_{440} = 66,000 M^{-1} cm^{-1} and two-photon cross section of 350 GM at 775 nm). We developed a "caged calcium" molecule by conjugation of BIST to a Ca^{2+} chelator that upon laser flash photolysis rapidly releases Ca^{2+} in less than 0.2 ms. Using the patch clamp method the optical probe enabled both one- and two-photon uncaging of Ca^{2+} inside acutely isolated rat cardiac myocytes that induced highly local or cell-wide physiological Ca^{2+} signaling events.

Introduction.

Photochemical uncaging of organic substrates is a valuable optical method that is used in many areas of science[1]. Invented by chemists for organic synthesis in the 1960s[2], it was adopted by physiologists in the 1970s[3] to control the concentration of cellular signaling molecules[4]. Material chemists have also found an important application of this method to construct high-density micro array chips[5]. Uncaging remains a uniquely powerful way to control the concentration of intracellular calcium ions ($[Ca^{2+}]_i$), but since covalent bonds cannot be made with ionized calcium, photolysis is normally used to decrease in an irreversible manner the affinity of Ca^{2+} chelators for the cation[6,7] (note sodium[8] and zinc[9] uncaging use our approach and that other approaches for Ca^{2+} have been suggested recently[10,11]). We have used the bifurcation of known high affinity tetracarboxylic molecules into known low affinity dicarboxylates for highly efficient rapid Ca^{2+} uncaging[12-14]. Because this is the only optical method for creating large changes in $[Ca^{2+}]_i$ of 10-100 μM, our optical probes have been extensively used for many biochemical and physiological experiments[15].

The most widely used chromophores for all uncaging experiments are the *ortho*-nitrobenzyl and *ortho*-nitroveratryl protecting groups, which absorb light in the near-ultraviolet range but are not efficiently photolyzed by visible light of longer wavelengths. Subsequently several chromophores have been used for uncaging of biological signaling molecules with blue light[16-21]. Photochemical protecting groups sensitive to green light have also been reported[22-24], but to our knowledge no biological studies have appeared with these probes. Some of these probes are very important additions to the arsenal of caged compounds available for use by biologists, however none of them offer the same generality of carbon-heteroatom bond scission that is part of *ortho*-nitrobenzyl photochemistry.

Extended π-electron systems have been used to tune the absorption maximum of fluorophores for one- and two-photon (or 1P and 2P) excitation[25-29]. However when these molecules are used for uncaging[25,27] they do not preserve the generality of simple *ortho*-nitrobenzyl groups. Thus, we have taken a step to address this need by creating an *ortho*-nitrobenzyl caging chromophore with an absorption maximum that is relatively bathochromic compared to the *ortho*-nitroveratryl chromophore. The new chromophore, a dinitro derivative of **bi**s**s**tyryl**t**hiophene (or BIST, blue substructure of **1** in **Fig. 1**), has a 1P absorption maximum at 440 nm (**Fig. 2a**), and is very sensitive to linear excitation

across the 400-500 nm range of the electromagnetic spectrum. Further, it has large 2P absorption cross-section, of at least 250 GM, in the 720-830 nm range (**Fig. 2b**). Here we detail the application of the BIST chromophore to the development of a photosensitive, Ca^{2+}-selective chelator based on ethyleneglycoltetraacetic acid (or EGTA)[30,31], which, with the addition of the cation becomes a caged calcium probe (**Fig. 1**) that is activated very efficiently by visible light.

Results

Chemical synthesis. Concerned about the lipophilic nature of the BIST chromophore, we chose as our first target a symmetrical molecule bearing two EGTA chelators. The synthesis of this molecule (**Fig. 1**), which we call BIST-2EGTA, started by conversion of 2-nitro-5-bromobenyzaldehyde into the epoxide with carboxymethyl-4-cyanophenylmethylsulfonium trifluoromethanesulfonate in presence of cesium carbonate to give **2** in a 74% yield. The diether backbone of the Ca^{2+} coordination sphere was created using base-catalyzed ring opening of the epoxide with ethylene glycol to give the desired diol **3** in 60% yield, along with 5% of the other regiomer. The mixture of diols was converted to their dibromides using Ph_3P and CBr_4. From this mixture pure dibromide **4** was easily isolated by flash chromatography and then treated with sodium azide to give **5** in 74% overall yield for the two steps. The vinyl unit was added to the chromophore by treatment of **5** with 2,4,6-trivinyl-boroxin pyridine complex and tetrakis(triphenylphosphine)palladium to give **6** in a yield of 73%. The complete chromophore was constructed by Heck coupling of **6** with dibromothiophene to give **7** in 71% yield. The ethyl ester of BIST-2EGTA was made by reduction of the tetraazide **7** to its tetraamine in 70% yield, followed by alkylation with ethyl bromoacetate to give octaester **8** in 44% yield. Finally, the esters were hydrolyzed with an excess of KOH to give the target chelator BIST-2EGTA (**1**). Importantly, we have found such solutions to be highly stable. Routinely store all caged compounds at -40ºC, and solutions of BIST-2EGTA have be found to be stable for more than one year, as judged by HPLC (same single peak). Furthermore, such solutions are equally efficacious when used for uncaging inside cells.

One- and two-photon absorption properties of BIST. Irradiation of BIST-2EGTA with visible light revealed that the new photosensitive chelator was photolyzed slightly more slowly than DEAC450-Glu (quantum yield 0.39[32]). Thus, HPLC analysis showed that BIST-2EGTA photolyzed with a quantum yield of photolysis of 0.23 (Supplemental Fig. 1 shows representative HPLC traces). The absorption maximum was bathochromically

shifted when compared to the widely used *ortho*-nitroveratryl photochemically protecting group (**Fig. 2a**), BIST-2EGTA shows peak absorption extinction coefficient at 440 nm with an extinction coefficient of 66,000 M^{-1} cm^{-1}. We used the z-scan method[33] and 2P-induced fluorescence (2PE) to determine the 2P absorption properties of simple BIST derivatives (**9**, **10**). We chose to examine molecules without benzylic substitutions for simplicity, as such functionalities would be photolyzed during such measurements. The simplest dinitro-BIST (**9**) had a 2P absorption cross section in DMSO of 740 GM at 775 nm. This chromophore absorbed 2 photons strongly across the 720-900 nm range (**Fig. 2b**). A BIST derivative having substituents *ortho* to both nitro groups (**10**) showed similar, large 2P absorption properties, with a maximum 2P cross section of 350 GM at 775 nm (**Fig. 2b**). Using the z-scan method we found a value of 390 GM at 775 nm for **10b** in DMSO, one that is not significantly different from the fluorescence determination. In water the 2P cross section of 775 nm of **10b** decreased to 250 GM. The 2-fold reduction of the 2P cross section of **9** is probably caused by steric clash between the *ortho* substituents and the nitro groups twisting the latter out of planarity with the aromatic ring system in compound **10**. The effects of the more polar aqueous solvent on the 2P cross section are consistent with other reports[34].

Calcium binding and release. Calcium titration of BIST-2EGTA in aqueous solution was used to determine the apparent dissociation constant at various pH vales. **Fig. 2c** shows the increase in fluorescence emission from X-rhod-1 during addition of defined aliquots of Ca^{2+} (0.1 mM) to a solution of BIST-2EGTA. These data allow the free [Ca^{2+}] to be determined as previously described[30], and showed that the chelator bound Ca^{2+} with high affinity (K_d 84 nM at pH 7.2, 50 nM at pH 7.35 and 19 nM at pH 7.5). In independent experiments we used Ca^{2+}-selective electrodes to measure and these data gave identical values for the K_d. The presence of physiological Mg^{2+} concentrations (i.e. 1 mM) had no effect on these values. Importantly, Ca^{2+} was shown to be a photoproduct of the BIST-2EGTA:Ca^{2+} complex upon irradiation with visible light. Photolysis of a solution of BIST-2EGTA 85% saturated with Ca^{2+} (1 mM cage with 1.7 mM Ca^{2+} at pH 7.35) with a blue laser (473 nm) increased the $[Ca^{2+}]_{free}$ from 0.2 μM to 20 μM measure with a Ca^{2+}-selective electrode. Modeling of this reaction with "Patcher's Power Tools" (see Supplemental Information) showed that the affinity changed approximately 20,000-fold. HPLC analysis showed 50% of BIST-2EGTA remained in this experiment (Supplemental Fig. 2). Note, the affinities of BIST-2EGTA before and after photolysis are very similar to the UV-light sensitive Ca^{2+} cage NP-EGTA[30,31].

Characterization of dynamic calcium uncaging. The rate of substrate release is important for many applications of caged compounds, especially those concerned with Ca^{2+} signaling[30]. Low affinity fluorescent Ca^{2+} dyes allow the monitoring of $[Ca^{2+}]$ to be measured as the rate-limiting step for equilibration of the dye:Ca^{2+} complex is determined by the off-rate of the dye[35]. Fluorescence imaging with a confocal microscope in point scan mode revealed that rhod-FF (K_d = 19 μM) showed a rapid change in signal (exponential time constant of less than 200 μs) when BIST-2EGTA was photolyzed using 2P excitation at 810 nm (**Fig. 2d**).

The widely used[15] nitroaromatic caged calcium compounds (e.g. DM-nitrophen[36] or NP-EGTA[31]) photolyze much more effectively at relatively short wavelengths (e.g. 2P excitation at 720 nm, or 1P excitation in the UV-C range) when compared to longer wavelengths (i.e. >800 nm for 2P excitation and 400-500 nm for 1P excitation). Thus DM-nitrophen showed a relative 2P uncaging efficacy of 7.40 for 720 nm versus 810 nm (**Fig. 2e**). Consistent with the 2P absorption spectrum (**Fig. 2d**), we found that BIST-2EGTA was equally sensitive to 2P photolysis at these two wavelengths (**Fig. 2f**). However, when DM-nitrophen was photolyzed under the same resting $[Ca^{2+}]_{free}$ the fluorescence signal from rhod-FF upon Ca^{2+} from BIST-2EGTA was about 13.7x larger than DM-nitrophen at 720 nm (**Fig. 2f**). (**Figs. 2e,f** also imply BIST is about 100x more effective at 810 nm.) Taken together these data show that BIST-2EGTA binds Ca^{2+} with high affinity, absorbs light strongly and is photolyzed efficiently to create changes in $[Ca^{2+}]$ that are potentially useful for physiological studies. We tested such effectiveness in acutely isolated cardiac myocytes.

Two-photon uncaging of Ca^{2+}: photocontrol of local Ca^{2+} signaling. In cardiac myocyte cells a small amount of Ca^{2+} enters the cytoplasm upon depolarization and initiates Ca^{2+}-induced Ca^{2+} release from the sarcoplasmic reticulum (SR) store, such release events can remain highly localized or initiate "Ca^{2+} waves" that propagate through the cell[37]. Individual myocytes were loaded with BIST-2EGTA (0.5 or 1 mM) and rhod-2 (0.1 mM) or X-rhod-5F (0.1 mM) via a patch pipette. 2P excitation at 810 nm produced localized Ca^{2+} transients that were considerably larger (**Fig. 3a**) than those produced by BIST-2EGTA photolysis in caffeine-treated cells (**Fig. 3b**, caffeine completely unloads Ca^{2+} from the SR, so allows the pure photolytic Ca^{2+} signal to be detected). Uncaging for longer periods triggered intracellular Ca^{2+} "mini-waves" that caused release events a small distance from the uncaging site (**Fig. 3c**). In contrast, we also found that very brief

irradiation of BIST-2EGTA for 1 ms could initiate highly localized Ca^{2+}-induced Ca^{2+} release from the SR (**Fig. 3d**). Previously we have found that with DM-nitrophen any release events always required substantially longer flash durations [13,14,38-40].

Photochemically initiated intracellular Ca^{2+} waves using visible light and 2P excitation. We found that 2P excitation of BIST-2EGTA could also initiation strong Ca^{2+}-induced Ca^{2+} release processes that extended considerable distances from the uncaging point. In **Fig. 4a** we show using 2D line scan fluorescence imaging that 2P excitation can produce such Ca^{2+} waves that propagate rapidly in both directions Note that such line scan imaging has the advantage of a very high imaging rate, 500 Hz, but conveys limited spatial information about the entire cardiac cell. Thus we combined visible light uncaging with full frame imaging which allowed us to produce striking Ca^{2+} waves that propagated throughout the cell (**Fig. 4b**). These signals are similar to those reported in many physiological studies of cardiac myocytes (reviewed in [37,41]). It should be noted there was negligible optical cross talk between the 810-nm 2P uncaging and 561-nm confocal imaging lasers under these conditions. Specifically, imaging at 561 nm was performed with energies 0.1% of those used for photolysis with 405 nm. Further, irradiation with EGTA in place of BIST-2EGTA or without prior chelator loading with Ca^{2+} did not produce any Ca^{2+} waves. Importantly, cells displayed normal excitation-contraction coupling, as seen in the cellular Ca^{2+} transient preceding photolytic Ca^{2+} release, implying that BIST-2EGTA is nontoxic inside cells (not shown).

Discussion.

We have developed an extended π–electron nitrobenzyl caging chromophore, which we call "BIST", that is photolyzed efficiently with visible light in the violet-blue region. Several recently developed caging chromophores are photolyzed in this range[1], however these cages are some what limited by the photosolvolysis reactions they use[32]. In contrast, the intramolecular photoredox reaction used by BIST not only uncages acids, but can also be used for carbon-amine and carbon-ether photoscission[42]. (See **Supplementary Fig. 3** where we show that amines and alcohols are uncaged cleanly from BIST.) We took advantage of this unique feature by using BIST to cleave a C-N tertiary amine bond at the heart of the Ca^{2+}-selective chelator EGTA to develop a caged Ca^{2+} probe that is photolyzed with visible light, and thus fabricate a caged Ca^{2+} probe with distinctive optical properties (Table 1).

Originally ultraviolet lasers were used to photolyze *ortho*-nitrobenzyl caged compounds rapidly[43,44]. Subsequently flash lamps with a filtered output were used[45,46]. However blue lasers are now much more widely available than either of these light sources, being standard on all confocal microscopes and used extensively for "optogenetics"[47]. Therefore the development of a new caging chromophore that is sensitive and efficiently photolyzed in this region of the electromagnetic spectrum is a potentially useful addition to the optical toolkit available to chemists and biologists. Having an extinction coefficient of 66,000 M^{-1} cm^{-1} it absorbs light very efficiently (c.f. fluorescein[48] has an extinction coefficient of 77,000 M^{-1} cm^{-1}), and strongly in the blue region, a property which is unique compared to other caged Ca^{2+} probes (Table 1). Furthermore 2P uncaging is also considerably more efficient than the *ortho*-nitroveratryl caging chromophore (**Fig. 2**), suggesting that direct attachment of a large 2P antenna to the caged substrate, rather than relying of resonance transfer[49], can be very effective for photorelease. Typically most extended π-electron systems examined by material chemists for 2P absorption are electron rich, with symmetrical diamino derivatives being very popular[50]. It is interesting that our electron deficient dinitro-BIST derivatives have similar 2P absorption properties to comparable diamino derivatives[51], suggesting that polarization *per s*e is the crucial property for chromophores in this context.

Conclusions.

BIST is a new photochemical protecting group that absorbs light efficiently. Beyond our initial application to Ca^{2+} uncaging, since BIST uses similar photochemistry to the widely used *ortho*-nitrobenzyl and *ortho*-nitroveratryl chromophores, we tentatively suggest BIST could be used to uncage the widest variety of functionalities. Our current data show that BIST-2EGTA is an exceptionally photosensitve caged Ca^{2+} probe (Table 1), making superb use of both 1P and 2P excitation. Importantly BIST-2EGTA is photolyzed by blue light and the wide availability of light sources in this region could make Ca^{2+} uncaging experiments attractive to many more laboratories.

Methods.

Chemical synthesis.
See supplement for full methods and analytic details.

Calcium affinity.
The Ca^{2+} affinity of BIST-2EGTA was measured as previously described by us for NP-EGTA[31]. Briefly, a home made Ca^{2+}-selective electrode was made using ETH-129. To a solution of BIST-2EGTA (0.5 – 1.0 mM) in HEPES (10 mM) and KCl (100 mM) was added incremental amounts (0.1 mM) of $CaCl_2$ and the change in $[Ca^{2+}]_{free}$ was measured. Scatchard analysis of such titrations revealed that at pH 7.2 the K_d was 82 nM, 50 nM at pH 7.35 and 19 nM at pH 7.5. Using the same homemade electrodes we found that the $[Ca^{2+}]_{free}$ of a solution of BIST-2EGTA (1 mM) with 1.7 mM $CaCl_2$ increased from 0.2 μM to 20 μM when 50% of the caged compound was photolyzed in a quartz cuvette with a 473nm-laser. In separate experiments we also used changes in fluorescence from X-rhod-1 to measure the $[Ca^{2+}]_{free}$. Values for the K_d using these methods were identical.

Quantum yield of photolysis.
The quantum yield of photolysis of BIST-2EGTA was measured as before[31,32]. Briefly, solutions of BIST-2EGTA and DEAC450-Glu, each with an optical density of 0.4 at 410 nm, were photolyzed with a 410 nm laser. The time-course of photolysis was followed by HPLC analysis. Each time point was analyzed thrice and the photolysis of each compound was also performed three times. The HPLC showed that the rate of photolysis of BIST-2EGTA was 60% of DEAC450-Glu with a 410-nm laser, implying a quantum yield of 0.23.

2P absorption cross-section.

The 2P absorption cross-section, δ (in GM = 1×10^{-50} cm^4 s $molecules^{-1}$ $photon^{-1}$), of the compounds examined was measured in the 730-930 nm wavelength range. We used the 2P-induced fluorescence (2PF) method[52] using 5-ns, 10-Hz pulses (compound **10**) and the z-scan technique using 60-fs, 1-kHz pulses (compound **9**). In 2PF experiment, an optical parametric oscillator laser (Spectra Physics, premiScan) pumped by a Q-switched Nd:YAG laser (Spectra Physics, Quanta-Ray Pro-250). The measurements were conducted in a regime where the fluorescence signal showed a quadratic dependence on

the intensity of the excitation beam. The fluorescence signal was collected by a lens and transferred via a fiber to a spectrometer (HORIBA Scientific, iHR320) with a CCD camera (HORIBA Scientific, Synapse). Coumarin 485 (ref[53], Sigma-Aldrich), rhodamine B, and bisstyrylbenzene (compound **8** in[54]), whose 2P properties have been well characterized in methanol, were used as the references in 2PF measurements. The samples were prepared in DMSO (Sigma-Aldrich, Spectrophotometric grade) at a concentration of 3-8×10^{-4} M and the optical pathlength of sample cuvettes for 2PF measurements was 1 cm. For z-scan measurements[55], an optical parametric amplified laser (Spectra Physics, TOPAS) pumped by a mode-locked Ti:sapphire regenerative amplifier system (Spectra Physics, Solstice) was used as the excitation source. The excitation beam for z-scan is spatially-filtered as a near Gaussian beam with $M^2 < 1.1$ and waist $\omega(HW_{1/e2}) \sim 40$ μm. The excitation irradiance ranged from 50-150 GW/cm^2. The samples were prepared in DMSO (ca. 2 mM) and the optical pathlength of sample cuvettes for z-scan measurements was 1 mm.

Laser flash photolysis in droplets.

A mode-locked Ti:sapphire laser (Mira 9000F, Coherent, Santa Clara, CA, USA) pumped by 8 W solid-state Verdi V-8 (Coherent) was used for 2P excitation of BIST-2EGTA or DM-nitrophen. Wavelength of the laser was set to 720 or 810 nm with pulse duration of ~120 fs. Power of the laser was adjusted by neutral density and polarizing filters and was measured at the objective focal plane by a power meter (PM200 with sensor S170C, Thorlabs, Newton, New Jersey, USA). Laser beam was guided to the SIM scanner of the confocal microscope (Fluoview 1000, Olympus, Volketswil, Switzerland) operating in single point excitation mode simultaneously with the main scanner. The photolysis period was 1 or 20 ms and the duration was controlled by an electronic shutter LS3 (Vincent Associates, Rochester, NY, USA) and triggered by the confocal microscope. The main scanner of confocal microscope was operating in the line scan mode. To record changes in Ca^{2+} concentration fluo-3, rhod-2 (both Biotium Inc., Hayward, CA, USA), X-rhod-5F (Life Technologies) or rhod-FF (Teflabs, Austin, TX, USA) were excited at 473 or 561 nm, respectively. Solutions used for droplet experiments were composed of (mM): for **Fig. 2b**: 1 BIST-2EGTA, 0.1 rhod-FF, 2 $CaCl_2$, 100 KCl, 10 HEPES, pH = 7.80; for **Fig. 2d**: 1 BIST-2EGTA, 0.1 rhod-FF, 2 $CaCl_2$, 100 KCl, 10 HEPES, pH = 8.0; for **Fig. 2c**: 2 DM-nitrophen, 0.5 $CaCl_2$, 0.1 fluo-3, 1 GSH, 5 K_2ATP, 10 HEPES, 20 TEA-Cl, 120 L-Aspartic acid, 120 CsOH, pH = 7.20; for **Fig. 2d**: 2 DM-nitrophen, 2 $CaCl_2$, 0.1 rhod-FF, 100 KCl, 10 HEPES, pH=7.20. Recorded images were analyzed in MATLAB (MathWorks, Inc., Natick, MA, USA) and Igor Pro (WaveMetrics, Inc., Portland, OR, USA).

Laser flash photolysis in cardiac myocytes.

Cardiac ventricular myocytes were isolated from C57Bl/6 mice as described before[56]. Myocytes were whole cell patched clamped at a resting potential -80 mV. A train of five to ten pre-pulses from -40 to 0 mV in the presence of 100 nM isoproterenol was applied to load the sarcoplasmic reticulum with Ca^{2+}. A photolytic pulse with a duration of 1-100 ms was applied 1-3 s after last conditioning pulse to release Ca^{2+} from BIST-2EGTA. For 2P photolysis we used an infrared laser with a wavelength of 810 nm, and for single photon photolysis we used a UV DPSS laser with wavelength 405 nm. Both laser beams were guided to the SIM scanner and data acquisition was the same as described above. Myocytes were placed in a recording chamber in external bath solution containing (mM): 140 NaCl, 5 KCl, 1 CsCl, 1.8 $CaCl_2$, 0.5 $BaCl_2$, 10 HEPES, 10 glucose, pH = 7.40. Pipettes were filled with internal solution containing (mM): for **Figs. 3a-e, 4a**: 0.5 BIST-2EGTA, 0.8 $CaCl_2$, 0.1 rhod-2, 1 GSH, 4 K_2ATP, 5 $MgCl_2$, 10 HEPES, 20 TEA-Cl, 120 L-Aspartic acid, 120 CsOH, 8 NaCl, pH = 7.50; for **Fig. 4b**: 1 BIST-2EGTA, 1.5 $CaCl_2$, 0.1 X-rhod-5F, 1 GSH, 5 K_2ATP, 10 HEPES, 20 TEA-Cl, 120 L-Aspartic acid, 120 CsOH, 8 NaCl, pH = 7.40. Images in **Figs. 3a-e, 4a** were normalized, filtered with Gaussian (kernel [5 5]) and Wiener filters (kernel [10 10]) and smoothed by cubic spline (p=0.5 in MATLAB "caps" function). Experiments were performed at room temperature. All recorded images were processed and analyzed in MATLAB, imageJ and Igor Pro.

Acknowledgements.
This work was supported by grants from the US NIH (GM053395 and NS069720) to GCRE-D, the AFOSR MURI (FA9550-10-10558) to JWP, and the Swiss National Science Foundation (31-156375 and the Microscopy Imaging Center, or "MIC") to EN. We would like to thank Drs. Simon Langenegger and Robert Häner for their help.

All authors commented on the paper and approved the final submitted version.

Supporting information. NMR spectra and HR-MS for all new compounds.

Notes.
The authors declare no competing financial interest.

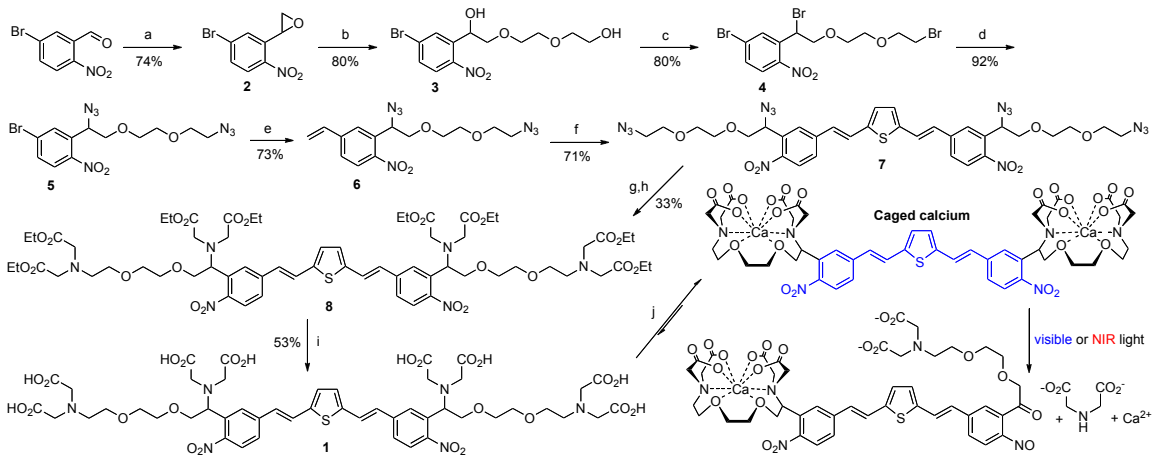

Figure 1. Synthesis of BIST-2EGTA.

Reagents and conditions: (a) Carboxymethyl-4-cyanophenylmethylsulfonium trifluoromethanesulfonate, Cs_2CO_3, THF; (b) diethylene glycol, NaH; (c) CBr_4, PPh_3, DCM; (d) NaN_3, NaI, DMF; (e) $Pd(PPh_3)_4$, 2,4,6-trivinyl-boroxin pyridine complex, K_2CO_3, DME, H_2O; (h) $Pd(OAc)_2$, LiCl, TBACl, $NaHCO_3$, DMF; (g) PPh_3, dioxane, NaOH (aq); (h) $BrCH_2COOEt$, pentamethylpiperidine, acetonitrile; (i) KOH, MeOH; (Note for clarity the counter cation not shown) (j) $CaCl_2$ in H_2O (Note for clarity the ionic valence and counter ion are not depicted).

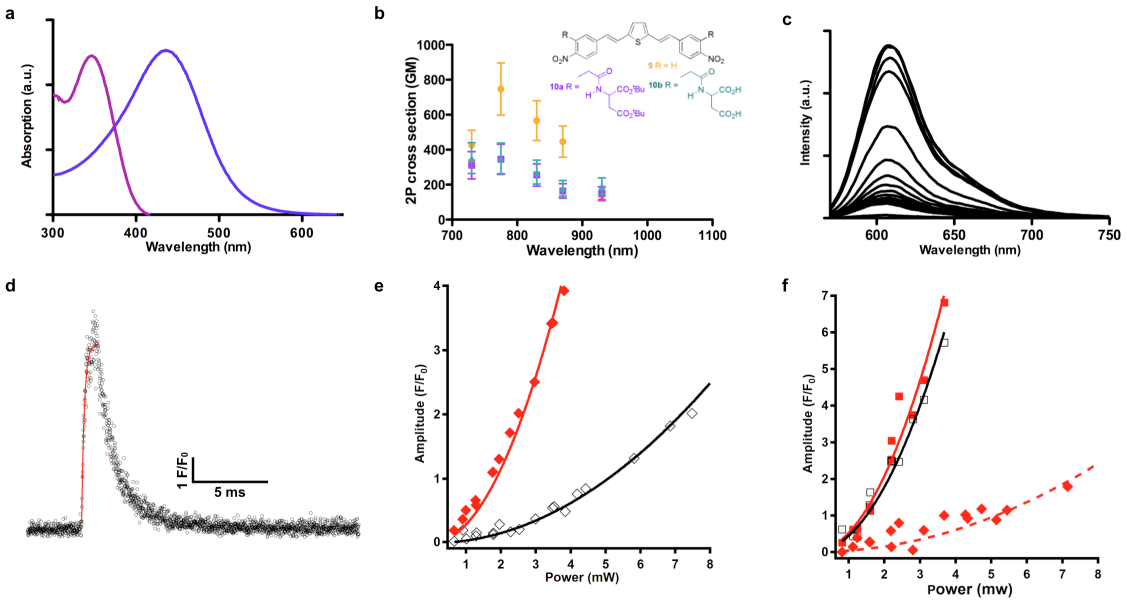

Figure 2. Photochemical characterization of BIST-2EGTA.

Non-linear absorption properties of BIST derivatives were measured using the z-scan technique or by 2P fluorescence emission. Rapid changes in $[Ca^{2+}]_{free}$ were monitored in point scan mode (10 μs per pixel) or in bidirectional line scanning mode (244 μs per line) using laser-scanning confocal microscopy at 561 or 473 nm after 2P photolysis with a mode-locked Ti:sapphire laser tuned to 810 or 720 nm.

(**a**) Absorption spectra of the BIST-2EGTA (blue) and *ortho*-nitroveratryl (DM-nitrophen, violet) chromophores showing their relative 1P maxima.

(**b**) 2P absorption spectra of BIST derivatives. Compound **9** had a 2P absorption maximum in DMSO of 740 GM at 775 nm (orange). Each data point is average of 5 or 6 measurements. Compounds **10a** (R purple) and **10b** (R green) have a 2P absorption maximum in DMSO of 350 GM at 775 nm. Each data point is an average of 3 for the three references compounds. All points are shown +/- SD.

(**c**) Example of Ca^{2+} titration of a solution of BIST-2EGTA with X-rhod-1. Addition of 0.1 mM amounts of $CaCl_2$ to a solution of BIST-2EGTA (0.5 mM) at pH 7.2 with KCl (100 mM) showed the chelator had a high pre-photolysis affinity for Ca^{2+}.

(**d**) 2P uncaging of BIST-2EGTA produced a rapid increase in Ca^{2+} monitored by point scan confocal imaging using rhod-FF. The exponential time-constant for the fluorescence increase was 164 μs.

(**e**) The relative efficacy of 2P uncaging of DM-nitrophen at 810 and 720 nm was determined by monitoring the photoreleased Ca^{2+} during a power train at these two wavelengths. Both wavelengths showed a quadratic dependence on incident power and

release was 7.4 +/- 0.23 times more effective at 720 nm (closed red diamonds) compared to 810 nm (open black diamonds). Fluo-3 was used to monitor Ca^{2+} release.
(**f**) Ca^{2+} release from BIST-2EGTA:Ca^{2+} complex at 810 and 720 nm was determined by monitoring the fluorescence signal from rhod-FF during a power train at these two wavelengths (810, open black squares; 720 closed red squares). The increase in fluorescence showed a quadratic dependence on incident power and was equally effective at both wavelengths. An identical power train was also used for photolysis of DM-nitrophen (720, closed red diamonds). The resting $[Ca^{2+}]_{free}$, the Ca^{2+}-bound and Ca^{2+}-free indicator concentrations were the same for both caged calcium compounds.

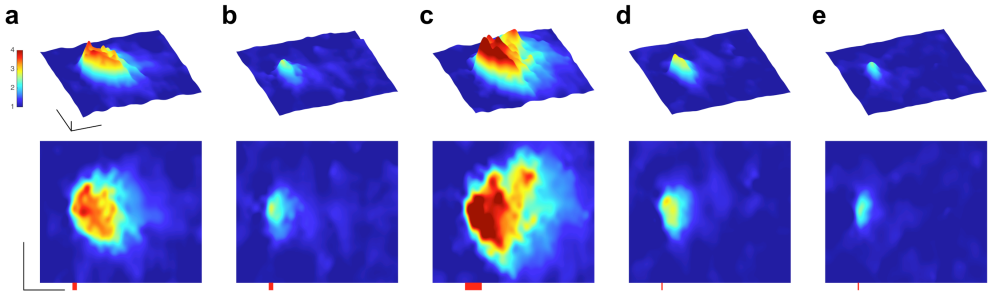

Figure 3. Localized control of Ca^{2+}-induced Ca^{2+} release in cardiac myocytes using 2P photolysis.

Single cardiac myocytes were loaded via a patch pipette with BIST-2EGTA and rhod-2. Changes in $[Ca^{2+}]_{free}$ were monitored in line scan mode (2.116 ms per line) using laser-scanning confocal microscopy at 561 nm after 2P uncaging at the center of the line with a mode-locked Ti:sapphire laser tuned to 810 nm. Line scan data are displayed as 3D surface plots (time in x, space in y and fluorescence as F/F_0 on a pseudo-color scale in z) with the corresponding 2D plots (time in x and distance in y) below each 3D panel. Scale bars are 1 F/F_0, 5 μm and 50 ms.

(**a**) Point 2P irradiation with 5 ms pulse (red bar) in cells triggered local Ca^{2+}-induced Ca^{2+} release from the SR.

(**b**) Photolysis of BIST-2EGTA produced highly spatially confined Ca^{2+} release. Cell was treated with caffeine (20 mM) to unload the Ca^{2+} from the SR.

(**c**) Increasing pulse duration to 20 ms initiated a Ca^{2+} "mini" wave, with discrete Ca^{2+} release events apparent beyond the initial uncaging location.

(**d**) Reducing pulse duration to 1 ms produced rapid, efficient and highly localized Ca^{2+}-induced Ca^{2+} release.

(**e**) Pure photolytic release of Ca^{2+} from BIST-2EGTA during irradiation for 1 ms (cell treated with caffeine as in **b**).

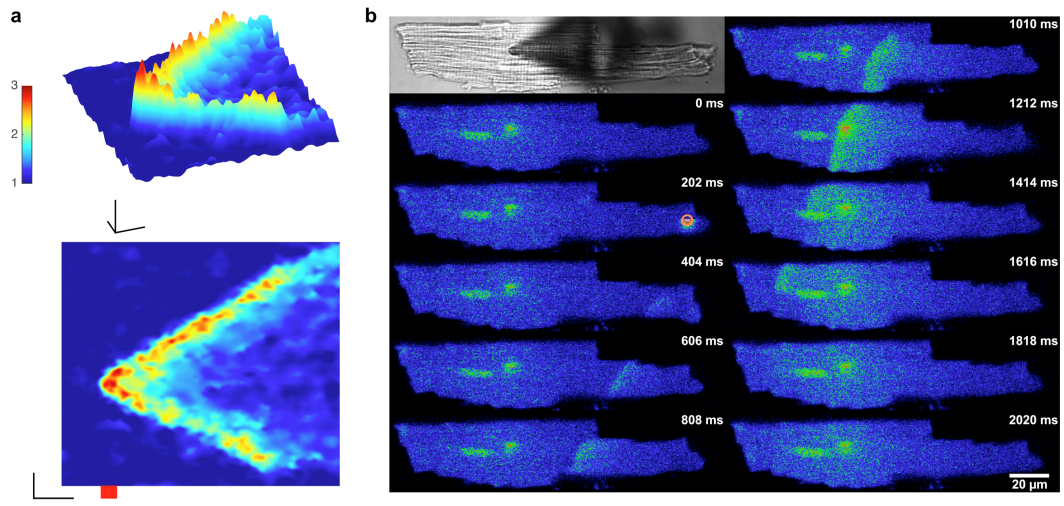

Figure 4. Visible light and 2P excitation of BIST-2EGTA:Ca^{2+} complex in cardiac myocytes initiates intracellular Ca^{2+} waves.

Single cardiac myocytes were loaded via a patch pipette with BIST-2EGTA and X-rhod-5F or rhod-2. Changes in $[Ca^{2+}]_{free}$ were monitored in line scan mode (2.116 ms per line) using laser-scanning confocal microscopy at 561 nm after 2P uncaging at the center of the line or by whole cell frame scan (202 ms per frame, 406 x 96 pixels) imaging after uncaging with visible light. A mode-locked Ti:sapphire laser tuned to 810 nm with 20 mW was used for 2P excitation. A 405-nm continuous-wave laser was used for uncaging with visible light (10 mW, 100 ms). Line scan data are displayed as 3D surface plots (time in x, space in y and fluorescence as F/F_0 on a pseudo-color scale in z) with the corresponding 2D plots (time in x and distance in y) below.

(**a**) Rapid line scan confocal imaging revealed 2P excitation (20 ms, red bar) could initiate Ca^{2+} signals that propagated extensively in both directions away from the initial uncaging position. Scale bars for units of 1 F/F_0, 5 μm and 50 ms.

(**b**) Uncaging with visible light (orange circle) initiated a Ca^{2+} wave that propagated throughout the cell. Top left is a transmitted light image of the cell with the pipette seen as a shadow. Pseudo-color images represent raw fluorescence intensity data. Frame sequence is top left to bottom left, followed by top right to bottom right. The nucleus and patch pipette can be seen in the left portion of the cell. The time stamp is from the beginning of each frame.

Probe	ϕ	ε_{max} (nm)	ε_{405} (nm)	ε_{473} (nm)	$\phi.\varepsilon_{max}$	2PCS (GM)	τ (μs)
nitr-5[57]	0.012	5,500 (350)	700	0	66	0.01	400
DM-nitrophen[36]	0.18	4,300 (350)	700	0	774	0.01	26
NP-EGTA[31]	0.23	975 (350*)	70	0	224	>0.001	15
azid-1[58]	1.0	33,000 (342)	840	0	33,000	1.0	2,000
NDBF-EGTA[14]	0.7	18,400 (330)	150	0	12,900	0.6	50
BIST-2EGTA	0.23	66,000 (440)	54,000	46,000	15,200	250	164

Table 1. Photochemical properties of caged Ca^{2+} probes. Symbols and notes: ϕ, quantum yield; ε, extinction coefficient; 2PCS, 2-photon cross section; τ, Ca^{2+} release time constant. *The ε_{max} for NP-EGTA is in the ultraviolet range.

References.

(1) Brieke, C.; Rohrbach, F.; Gottschalk, A.; Mayer, G.; Heckel, A. *Angew Chem Int Edit* **2012**, *51*, 8446-76.

(2) Barltrop, J. A.; Plant, P. J.; Schofield, P. *Chem. Commun.* **1966**, 822-3.

(3) Kaplan, J. H.; Forbush, B.; Hoffman, J. F. *Biochemistry* **1978**, *17*, 1929-35.

(4) Ellis-Davies, G. C. R. *Nat Methods* **2007**, *4*, 619-28.

(5) McGall, G. H.; Barone, A. D.; Diggelmann, M.; Fodor, S. P. A.; Gentalen, E.; Ngo, N. *J. Am. Chem. Soc.* **1997**, *119*, 5081-5090.

(6) Adams, S. R.; Tsien, R. Y. *Annu Rev Physiol* **1993**, *55*, 755-84.

(7) Ellis-Davies, G. C. *Methods Enzymol* **2003**, *360*, 226-38.

(8) Warmuth, R.; Grell, E.; Lehn, J. M.; Bats, J. W.; Quinkert, G. *Helv Chim Acta* **1991**, *74*, 671-681.

(9) Basa, P. N.; Antala, S.; Dempski, R. E.; Burdette, S. C. *Angew Chem-Int Ed* **2015**, *54*, 13027-13031.

(10) Wu, L.; Dai, Y.; Marriott, G. *Org Lett* **2011**, *13*, 2018-21.

(11) Li, D.; Hérault, K.; Isacoff, E. Y.; Oheim, M.; Ropert, N. *J Physiol (Lond)* **2012**, *590*, 855-73.

(12) Ellis-Davies, G. C. R.; Kaplan, J. H.; Barsotti, R. J. *Biophys J* **1996**, *70*, 1006-16.

(13) DelPrincipe, F.; Egger, M.; Ellis-Davies, G. C.; Niggli, E. *Cell Calcium* **1999**, *25*, 85-91.

(14) Momotake, A.; Lindegger, N.; Niggli, E.; Barsotti, R. J.; Ellis-Davies, G. C. *Nat Methods* **2006**, *3*, 35-40.

(15) Ellis-Davies, G. C. R. *Chem Rev* **2008**, *108*, 1603-1613.

(16) Amatrudo, J. M.; Olson, J. P.; Agarwal, H. K.; Ellis-Davies, G. C. R. *Eur J Neurosci* **2015**, *41*, 5-16.

(17) Chiu, C. Q.; Lur, G.; Morse, T. M.; Carnevale, N. T.; Ellis-Davies, G. C. R.; Higley, M. J. *Science* **2013**, *340*, 759-62.

(18) Rial Verde, E. M.; Zayat, L.; Etchenique, R.; Yuste, R. *Front. Neural Circuits* **2008**, *2*, 2.

(19) Olson, J. P.; Banghart, M. R.; Sabatini, B. L.; Ellis-Davies, G. C. R. *J Am Chem Soc* **2013**, *135*, 15948-54.

(20) Priestman, M. A.; Shell, T. A.; Sun, L.; Lee, H.-M.; Lawrence, D. S. *Angew Chem Int Edit* **2012**, *51*, 7684-7.

(21) Fournier, L.; Gauron, C.; Xu, L.; Aujard, I.; Le Saux, T.; Gagey-Eilstein, N.; Maurin, S.; Dubruille, S.; Baudin, J. B.; Bensimon, D.; Volovitch, M.; Vriz, S.; Jullien, L. *ACS Chem Biol* **2013**, *8*, 1528-36.

(22) Goswami, P. P.; Syed, A.; Beck, C. L.; Albright, T. R.; Mahoney, K. M.; Unash, R.; Smith, E. A.; Winter, A. H. *J Am Chem Soc* **2015**, *137*, 3783-3786.

(23) Rubinstein, N.; Liu, P.; Miller, E. W.; Weinstain, R. *Chem Commun* **2015**, *51*, 6369-6372.

(24) Umeda, N.; Takahashi, H.; Kamiya, M.; Ueno, T.; Komatsu, T.; Terai, T.; Hanaoka, K.; Nagano, T.; Urano, Y. *ACS Chem Biol* **2014**, *9*, 2242-2246.

(25) Zhou, W.; Kuebler, S. M.; Braun, K. L.; Yu, T.; Cammack, J. K.; Ober, C. K.; Perry, J. W.; Marder, S. R. *Science* **2002**, *296*, 1106-9.

(26) Hara, K.; Sato, T.; Katoh, R.; Furube, A.; Ohga, Y.; Shinpo, A.; Suga, S.; Sayama, K.; Sugihara, H.; Arakawa, H. *J. Phys. Chem. B* **2003**, *107*, 597-606.

(27) Gug, S.; Bolze, F.; Specht, A.; Bourgogne, C.; Goeldner, M.; Nicoud, J.-F. *Angew Chem Int Edit* **2008**, *47*, 9525-9529.

(28) Albota, M.; Beljonne, D.; Bredas, J.; Ehrlich, J.; Fu, J.; Heikal, A.; Hess, S.; Kogej, T.; Levin, M.; Marder, S.; McCord-Maughon, D.; Perry, J.; Rockel, H.; Rumi, M.; Subramaniam, C.; Webb, W.; Wu, X.; Xu, C. *Science* **1998**, *281*, 1653-1656.

(29) Reinhardt, B.; Brott, L.; Clarson, S.; Dillard, A.; Bhatt, J.; Kannan, R.; Yuan, L.; He, G.; Prasad, P. *Chem Mater* **1998**, *10*, 1863-1874.

(30) Ellis-Davies, G. C. R.; Barsotti, R. J. *Cell Calcium* **2006**, *39*, 75-83.

(31) Ellis-Davies, G. C. R.; Kaplan, J. H. *Proc Natl Acad Sci U S A* **1994**, *91*, 187-91.

(32) Olson, J. P.; Kwon, H. B.; Takasaki, K. T.; Chiu, C. Q.; Higley, M. J.; Sabatini, B. L.; Ellis-Davies, G. C. R. *J Am Chem Soc* **2013**, *135*, 5954-7.

(33) Thorley, K. J.; Hales, J. M.; Kim, H.; Ohira, S.; Bredas, J. L.; Perry, J. W.; Anderson, H. L. *Chemistry-a European Journal* **2013**, *19*, 10370-10377.

(34) Woo, H. Y.; Liu, B.; Kohler, B.; Korystov, D.; Mikhailovsky, A.; Bazan, G. C. *J Am Chem Soc* **2005**, *127*, 14721-14729.

(35) Higley, M. J.; Sabatini, B. L. *Neuron* **2008**, *59*, 902-13.

(36) Kaplan, J. H.; Ellis-Davies, G. C. R. *Proc Natl Acad Sci U S A* **1988**, *85*, 6571-5.

(37) Niggli, E. *Annu Rev Physiol* **1999**, *61*, 311-35.

(38) Lipp, P.; Niggli, E. *J Physiol* **1998**, *508 (Pt 3)*, 801-9.

(39) Lindegger, N.; Niggli, E. *J Physiol* **2005**, *565*, 801-13.

(40) Ogrodnik, J.; Niggli, E. *J Physiol (Lond)* **2010**, *588*, 225-42.

(41) Cheng, H.; Lederer, W. J. *Physiol Rev* **2008**, *88*, 1491-545.

(42) Binkley, R. W.; Flechtner, T. W. In *Synthetic Organic Photochemistry*; Horspool, W. M., Ed.; Plenum: New York and London, 1984, p 375-423.

(43) McCray, J. A.; Herbette, L.; Kihara, T.; Trentham, D. R. *Proc Natl Acad Sci U S A* **1980**, *77*, 7237-41.

(44) Goldman, Y. E.; Hibberd, M. G.; McCray, J. A.; Trentham, D. R. *Nature* **1982**, *300*, 701-5.

(45) Rapp, G.; Poole, K. J. V.; Maeda, Y.; Ellis-Davies, G. C. R.; Kaplan, J. H.; Mccray, J.; Goody, R. S. *Berichte Der Bunsen-Gesellschaft-Physical Chemistry Chemical Physics* **1989**, *93*, 410-415.

(46) Nerbonne, J. M.; Richard, S.; Nargeot, J.; Lester, H. A. *Nature* **1984**, *310*, 74-6.

(47) Gradinaru, V.; Thompson, K. R.; Zhang, F.; Mogri, M.; Kay, K.; Schneider, M. B.; Deisseroth, K. *J Neurosci* **2007**, *27*, 14231-8.

(48) Sjoback, R.; Nygren, J.; Kubista, M. *Spectrochimica Acta Part a-Molecular and Biomolecular Spectroscopy* **1995**, *51*, L7-L21.

(49) Cueto Diaz, E. J.; Picard, S.; Chevasson, V.; Daniel, J.; Hugues, V.; Mongin, O.; Genin, E.; Blanchard-Desce, M. *Org Lett* **2015**, *17*, 102-5.

(50) Rumi, M.; Barlow, S.; Wang, J.; Perry, J. W.; Marder, S. R. *Adv Polym Sci* **2008**, *213*, 1-95.

(51) Zheng, S.; Beverina, L.; Barlow, S.; Zojer, E.; Fu, J.; Padilha, L. A.; Fink, C.; Kwon, O.; Yi, Y.; Shuai, Z.; Van Stryland, E. W.; Hagan, D. J.; Bredas, J. L.; Marder, S. R. *Chem Commun (Camb)* **2007**, 1372-4.

(52) Pond, S. J. K.; Rumi, M.; Levin, M. D.; Parker, T. C.; Beljonne, D.; Day, M. W.; Bredas, J. L.; Marder, S. R.; Perry, J. W. *Journal of Physical Chemistry A* **2002**, *106*, 11470-11480.

(53) Makarov, N. S.; Drobizhev, M.; Rebane, A. *Optics Express* **2008**, *16*, 4029-4047.

(54) Rumi, M.; Ehrlich, J. E.; Heikal, A. A.; Perry, J. W.; Barlow, S.; Hu, Z. Y.; McCord-Maughon, D.; Parker, T. C.; Rockel, H.; Thayumanavan, S.; Marder, S. R.; Beljonne, D.; Bredas, J. L. *J. Am. Chem. Soc.* **2000**, *122*, 9500-9510.

(55) Powell, C. E.; Morrall, J. P.; Ward, S. A.; Cifuentes, M. P.; Notaras, E. G. A.; Samoc, M.; Humphrey, M. G. *J. Am. Chem. Soc.* **2004**, *126*, 12234-12235.
(56) Ullrich, N. D.; Fanchaouy, M.; Gusev, K.; Shirokova, N.; Niggli, E. *Am J Physiol Heart Circ Physiol* **2009**, *297*, H1992-2003.
(57) Adams, S. R.; Kao, J. P. Y.; Grynkiewicz, G.; Minta, A.; Tsien, R. Y. *J Am Chem Soc* **1988**, *110*, 3212-3220.
(58) Adams, S. R.; Lev-Ram, V.; Tsien, R. Y. *Chem Biol* **1997**, *4*, 867-78.